doi: 10.4149/gpb_2019050

Tripterine emerges as a potential anti-scarring agent in NIH/3T3 cells by repressing *ANRIL*

Lei Jiang*, Junjun Sun* and Peng Wang

Department of Aesthetic, Plastic, and Burn Surgery, Yuhuangding Hospital Affiliated Hospital of Qingdao University, Yantai City, Shandong Province, China

Abstract. Extensive scarring normally causes hypertrophic or keloid scars. This intuitively results in psychosocial distress and reduction in life quality. Tripterine is a bioactive pentacyclic triterpenoid compound while it is still poorly understood whether it possesses an anti-scarring function. NIH/3T3 cells were administrated with tripterine at increased concentrations (0–10 μM). Antisense RNA to INK4 locus (*ANRIL*) was transformed into NIH/3T3 cells, and the cells transfected with empty vector (mock transfection) were used as negative control. Then, cell viability and migration were profiled by cell counting kit-8 (CCK-8) and 24-Transwell assay. Protein expression was analyzed by Western blot assay. *ANRIL* was quantified by quantitative reverse transcription-PCR (qRT-PCR). Tripterine administration induced the growth inhibition of NIH/3T3 cells indicated by a trend toward the decreased expression of matrix metallopeptidase (*MMPs*), vascular endothelial growth factor (*VEGF*) and basic fibroblast growth factor (*bFGF*). This process was accompanied by the decreased phosphorylation of p65, inhibitor of nuclear factor kappa-B alpha (IκBα) and the downregulation of β-catenin. Moreover, *ANRIL* expression was notably repressed by tripterine. By contrast, in *ANRIL*-transfected cells, the effect of tripterine was abolished. Tripterine exhibited an anti-scarring bioactivity in NIH/3T3 cells by inhibiting *ANRIL*, and this process was accompanied by the blockade of nuclear factor-kappa B (NF-κB) and β-catenin cascades.

Key words: Antisense RNA to INK4 locus — NF-κB — β-catenin — Scarring

Introduction

Scar tissue is a type of cellular fibrotic matrix, which contributes to the manifestation and progression of a myriad of diseases when it occurs in heart (Furtado et al. 2016) and kidney (Salvatore et al. 2013), although it aids regeneration in some contexts, such as central nervous system axon regeneration (Anderson et al. 2016). Mostly, injury to skin generates a wound, which is normally irreversible and eventually evokes the formation of scar, a physical and chemical barrier for regeneration, with a disfiguring condition. For patients, these visible scars definitely and intuitively cause psychosocial distress and sacrifice quality of life (Verma et al. 2014; Finnerty et al. 2016). As a consequence, better approaches are currently required to reduce scarring, which are supposed to have substantial clinical efficacy.

During wound repairing progress, fibroblasts are recruited into extracellular matrix (ECM), proliferate in response to cytokines and synthesize ECM molecules which are implicated in restoration of structure and function. Mostly, severe scarring, such as hypertrophic or keloid scars, is characterized by high proliferation of fibroblasts and imbalance between collagen synthesis and degradation (Keane et al. 2018). Particularly, matrix metalloproteinases (MMPs) are described to be essential for wound healing because of the function in re-epithelialization, scarring and clearance (Rohani et al. 2015). Correspondingly, it has been proposed that the cellular therapy, based on matrix control, might assist in reducing scarring (Sidgwick et al. 2012).

Antisense RNA to INK4 locus is identified as long noncoding RNA and generally marked as *ANRIL*. It has been

* These authors contributed equally to this work.

Correspondence to: Peng Wang, Department of Aesthetic, Plastic, and Burn Surgery, Yuhuangding Hospital Affiliated Hospital of Qingdao University, No. 20 Yuhuangding East Road, Yantai City, Shandong Province, China
E-mail: wang71wp@sina.com

associated with atherosclerosis (Holdt et al. 2016), cancers (Naemura et al. 2015) and diabetic retinopathy (Thomas et al. 2017). Intriguingly, a recent study found the enhancement of ECM proteins and vasoactive factors is suppressed in *ANRIL*-knockout diabetic animals (Thomas et al. 2018). It is well-known that scarring presents perturbation between spatiotemporal accumulation and degradation of ECM (Keane et al. 2018). Particularly, Zhou et al. (2016) found tumor necrosis factor alpha (TNF-α) induced the abundance of *ANRIL* by activating nuclear factor-kappa B (NF-κB) of which the key subunit p65 increasingly binds to the promoter of *ANRIL*; subsequently, *ANRIL* mediates the expression of inflammatory genes downstream of *TNF-α* by interacting with transcriptional factor which is guided onto the corresponding promoter sites.

Tripterine (its chemical structure as shown in Fig. 1), known as celastrol, is a bioactive pentacyclic triterpenoid compound which had been detected in traditional Chinese medicinal herb *Tripterygium wilfordii,* Hook F. Clinically, *Tripterygium wilfordii,* Hook F is approved to treating rheumatoid arthritis, and the monotherapy shows a good efficacy according to the results from follow-up visit (Lv et al. 2015; Zhou et al. 2018). It is a potent antioxidant evidenced by inhibiting lipid peroxidation (Bian et al. 2016) and an anti-inflammatory agent by balancing pathogenic and regulatory T cells (Astry et al. 2015). What's more, it exhibits an anti-cancer capacity evidenced by anti-angiogenic properties (Gao et al. 2019). However, there are few reports that tripterine has shown clinical activity in scarring formation. As a consequence, we investigated the potential roles of tripterine in scarring. Besides, a further proof-of-principle study is performed in our study.

To further evaluate the potential function of tripterine as an anti-scarring agent, we examined the cellular and ECM alteration in NIH/3T3 cells. Moreover, we applied the *ANRIL*-transfected NIH/3T3 system to investigate the molecular underpinnings.

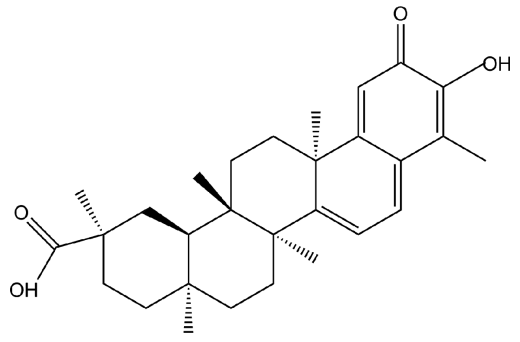

Figure 1. Chemical structure of tripterine (CAS 34157-83-0). Molecular formula, $C_{29}H_{38}O_4$; average mass, 450.610; synonym, celastrol.

Materials and Methods

Cell culture and administration

Fibroblast NIH/3T3 cells (Product No., CRL-1658^{TM}) (American Type Culture Collection) (ATCC) (Rockville, MD, USA) were grown in Dulbecco's modified Eagle's medium (Gibco, Gaithersburg, MD, USA) containing 10% fetal bovine serum (FBS) (Gibco) and 1% penicillin-streptomycin (Sigma-Aldrich, St. Louis, MO, USA) and were maintained in a humidified incubator containing 95% air and 5% CO_2 at 37°C. According to the information from the supplier, NIH/3T3 cells were derived from the embryo of NIH/Swiss mouse. Tripterine (Product No., C0869, Sigma-Aldrich), with a purity more than 98% at high performance liquid chromatography (HPLC) grade, was dissolved and stocked in dimethylsulfoxide (DMSO) (Sigma-Aldrich) at a concentration of 1 mM and then diluted into a series of concentration at 2, 4, 6, 8 and 10 μM. NIH/3T3 cells were co-incubated with tripterine for 4 h.

Cell viability analysis

Cell viability was evaluated by using a convenient and commercial kit, cell counting kit-8 (CCK-8) (APExBIO, Houston, TX, USA). It is based on a mechanism, that is, 2-(2-methoxy-4-nitrophenyl)-3-(4-nitrophenyl)-5-(2,4-disulfophenyl)-2H-tetrazolium monosodium salt is reduced by dehydrogenases in viable cells into formazan, which can be detected by a Microplate reader at 450 nm, in the presence of electron mediator. Briefly, NIH/3T3 cell suspension (100 μl) was inoculated in 96-well plates in a density of 5,000 cells *per* well. After pre-incubation for 24 h, NIH/3T3 cells were co-incubated with tripterine at a concentration of 2–10 μM for 4 h with a control group in which NIH/3T3 cells were administrated with culture medium containing an equivalent concentration of DMSO (less than 1‰). Each well was added with 10 μl of CCK-8 solution and continually incubated for 1 h. Finally, the absorbance was read using a Varioskan LUX Multimode Microplate Reader under 450 nm (Thermo Fisher Scientific, Waltham, MA, USA). Cell viability was depicted as the percentage of the control group.

Transfection

To enforce the up-regulation of *ANRIL* (GenBank No., AB548314.1) in NIH/3T3 cells, MIH/3T3 cells were transfected with *ANRIL*. Shortly, the full sequence of *ANRIL* (the sequence information was available on https://www.ncbi.nlm.nih.gov/nuccore/AB548314.1) was ligated into pcDNATM3.1/V5-His-TOPO vector (Invitrogen, Carlsbad, CA, USA). Plasmids transfection was performed using Lipofectamine 2000 transfection reagent (Invitrogen). Then, the cells were incubated in the culture medium in the

presence of G418 (0.5 mg/ml; Invitrogen). The transfection efficiency was finally identified using quantitative reverse transcription-PCR (qRT-PCR).

Migration analysis

To assay migration behaviors of NIH/3T3 cells, a transwell chamber (BD Biosciences, Bedford, USA) was applied in our study. In short, NIH/3T3 cell were inoculated onto the upper compartment at density of 30,000 cells *per* filter after administration. The bottom wells were filled with medium. After 24 h of culture, the non-migrated cells in the upper surface of the filter were gently scraped with a cotton swab. Meanwhile, the cells on the lower surface were stained with crystal violet. Then, the absorbance was detected using a Microplate reader at 540 nm. Data was presented as the percentage of migration relative to the control.

qRT-PCR assay

Total RNA was isolated from NIH/3T3 cells using RNeasy Plus Micro kit (QIAGEN, Hilden, Germany). To obtain cDNA, reverse transcription was conducted with Oligo(dT)$_{20}$ primers (Invitrogen). Next, PCR was carried out using SYBR Green PCR Master Mix (Applied Biosystems, Foster City, CA, USA) with specific primers of *ANRIL*, forward 5'-TGC TCT ATC CGC CAA TCA GG-3', reverse 5'-GGG CCT CAG TGG CAC ATA CC-3'. Reaction was conducted triply on a QuantStudio 3 Real-Time PCR system (Applied Biosystems). The expression of *ANRIL* was normalized to GAPDH with $2^{-\Delta\Delta CT}$ method.

Western blotting assay

Protein expression was assayed by Western blotting assay. Firstly, total proteins were extracted from the cells using RIPA lysis buffer (Beyotime, Shanghai, China) supplemented with protease and phosphatase inhibitors (Roche Applied Science, Indianapolis, USA). Then, the supernatant was obtained after centrifugation (15,000 rpm, 20 min) and protein concentration was evaluated using BCA^{TM} protein assay kit (Pierce, Appleton, WI, USA). Next, protein separation and transference were achieved using a Bio-Rad V3 Western Blot Workflow (Bio-Rad, Hercules, CA, USA). The polyvinylidene difluoride (PVDF) membranes (Millipore, Bedford, MA, USA) carrying protein imprints were blocked with bovine serum albumin (BSA) (Thermo Fisher Scientific) for 1 h at room temperature, followed by co-incubation with primary antibodies against cyclin D1 (ab16663; Abcam, Cambridge, MA, USA; 1:100), MMP-2 (87809; Cell Signaling Technology, CST, Danvers, MA, USA; 1:1,000), MMP-9 (ab38898; Abcam; 1:1,000), vascular endothelial growth factor (VEGF) (MAB4931; R&D Systems, Abingdon, UK; 1 μg/ml), basic fibroblast growth factor (bFGF) (NBP1-18579; Novus Biologicals, Colombia, USA; 1:1,000), β-actin (4967; CST; 1:1,000), total-p65 (8242; CST; 1:1,000), phospho (p) Ser536-p65 (3033; CST; 1:1,000), total-inhibitor of nuclear factor kappa-B alpha (IκBα) (4812; CST; 1:1,000), pSer32-IκBα (2859; CST; 1:1,000). Then the primary antibodies were probed by secondary antibodies, goat anti-rabbit (7074; CST; 1:5,000) and anti-rat (ab97057; CST; 1:5,000) IgG conjugated by horseradish peroxidase. Finally, an enhanced chemiluminescence agent was exploited for the visualization of protein bands on ChemiDoc^{TM} MP Imaging System (Bio-Rad) with a quantification using Image Lab^{TM} software (Bio-Rad).

Statistical analysis

Each experiment was carried out in triple using three independent performances. All data was presented as the mean ± standard deviation (SD). *p*-values were calculated by two-tailed Student's-*t* test and one-way analysis of variance (ANOVA) followed by Bonferroni's test using GraphPad Prism 6.0 software (GraphPad, San Diego, CA, USA). The significance was statistically considered when *p*-values were less than 0.05.

Results

Tripterine weakened cell viability and migration with the decline of cyclin D1, MMPs, VEGF and bFGF

To confirm the effect of tripterine on NIH/3T3 cells, we incubated the cells with tripterine at different concentrations (2–10 μM). Apparently, tripterine reduced ($p < 0.05$) cell viability with a dose-response manner (4–10 μM) while a not significant alteration of cell viability was observed at a concentration of 2 μM ($p > 0.05$) as shown in Fig. 2A. After 4 h of treatment with 6 μM tripterine, around 50% of NIH/3T3 cells remained ($p < 0.01$) obviously viable compared to un-treated cells (Fig. 2A). Consequently, further studies were carried out with NIH/3T3 cells administrated by 6 μM tripterine. Our results showed that NIH/3T3 cells treated with tripterine showed the notable blockade of ($p < 0.01$) migration (Fig. 2B) and significant reduced expression of ($p < 0.01$) cyclin D1 (Fig. 2C), (both $p < 0.05$) MMPs (MMP-2 and MMP-9) (Fig. 2D), ($p < 0.01$) VEGF and ($p < 0.01$) bFGF (Fig. 2E). Collectively, tripterine exhibited a potential suppressive role in scar formation.

Tripterine decreased expression of ANRIL

In the present study, NIH/3T3 cells were pre-incubated with 6 μM tripterine for 4 h and then examined for *ANRIL*

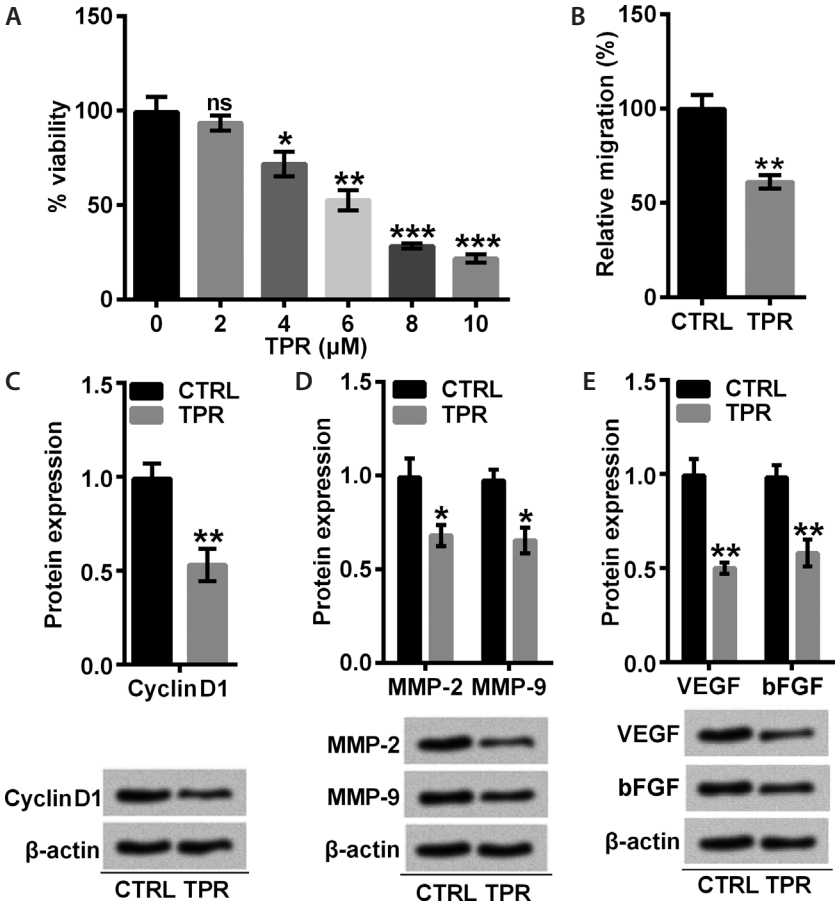

Figure 2. Effect of tripterine treatment on growth of NIH/3T3 cells. **A.** Cell viability of NIH/3T3 cells after tripterine (2–10 μM, treatment for 4 h) administration by cell counting kit-8 assay. **B.** Migratory NIH/3T3 cells after tripterine (6 μM, treatment for 4 h) by 24-Transwell assay. Protein expression of Cyclin D1 (**C**), MMP-2 and MMP-9 **(D)** as well as VEGF and bFGF **(E)** in NIH/3T3 cells treated with 6 μM tripterine for 4 h assayed by Western blot assay. Data represented means ± SD. ^{ns} $p > 0.05$, * $p < 0.05$, ** $p < 0.01$, *** $p < 0.001$. TPR, tripterine; CTRL, control; MMP, matrix metallopeptidase; VEGF, vascular endothelial growth factor; bFGF, basic fibroblast growth factor.

mRNA level. The results showed that after administration, NIH/3T3 cells showed ($p < 0.01$) a remarked increase in *ANRIL* expression (Fig. 3). This raised a hypothesis whether tripterine could repress cell viability and migration as well as attenuate the accumulation of cyclin D1, MMPs, VEGF and bFGF by down-regulating *ANRIL*.

ANRIL served as a negative mediator for tripterine during repressing the growth of NIH/3T3 cells

NIH/3T3 cells were stably transfected with human *ANRIL* gene and selected in G418-supplemented medium. Obviously, a notable overexpression ($p < 0.01$) of *ANRIL* was observed in *ANRIL*-transfected cells (Fig. 4A). As indicated, evaluation of *ANRIL*-overexpressed NIH/3T3 cells treated with tripterine exhibited a trend toward visibly ($p < 0.05$) enhanced cell viability (Fig. 4B) and ($p < 0.05$) increased expression of cyclin D1 (Fig. 4C). In addition, the migration behavior was ($p < 0.05$) evidently fortified (Fig. 4D). What's more, *ANRIL*-transfected NIH/3T3 cells showed a prominent accumulation of ($p < 0.01$) MMP-2, ($p < 0.01$) MMP-9 (Fig. 4E) though the cells were pre-incubated with tripterine. Consistently, the overexpression of VEGF ($p < 0.01$) and bFGF ($p < 0.01$) was detected in *ANRIL*-overexpressed NIH/3T3 cells in spite of tripterine treatment (Fig. 4F). All these results illuminated that tripterine might block the growth of fibroblast NIH/3T3 cells by down-regulating *ANRIL*.

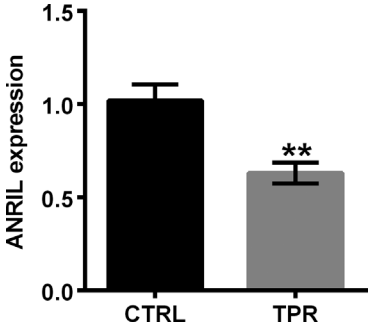

Figure 3. Effect of tripterine on *ANRIL* expression of NIH/3T3 cells. *ANRIL* mRNA level in NIH/3T3 cells administrated with 6 μM tripterine for 4 h evaluated by qRT-PCR. Data represented means ± SD after normalization with GAPDH. ** $p < 0.01$. CTRL, control; TPR, tripterine; *ANRIL*, antisense noncoding RNA in the INK4 locus; qRT-PCR, quantitative reverse transcription-PCR; GAPDH, glyceraldehyde-3-phosphate dehydrogenase.

Tripterine blunted NF-κB and β-catenin signaling pathways by down-regulating ANRIL

To get a better picture of its effects on associated signaling transduction cascades, we evaluated NF-κB and β-catenin signaling pathways. As shown in Fig. 5A, tripterine resulted in a down-regulation in phosphorylated expression of ($p < 0.05$) p65 and ($p < 0.05$) IκBα in NIH/3T3 cells, whereas *ANRIL* overexpression contributed to the phosphorylation of ($p < 0.01$) p65 and ($p < 0.05$) IκBα, suggesting that tripterine might blunt NF-κB cascade by repressing *ANRIL*. Moreover, our results indicated that tripterine, which ($p < 0.05$) broadly down-regulated β-catenin expression, was actually ($p < 0.01$) up-regulated its level in *ANRIL*-overexpressed cells (Fig. 5B). In fact, this up-regulation might be ascribed to *ANRIL* overexpression. Taken together, tripterine might blunt NF-κB and β-catenin transduction cascades *via* down-regulating *ANRIL*.

Discussion

A recent study showed an efficient inhibitory role of tripterine in the formation of erythema and scaling by decreasing the level of cytokines in psoriasis mouse models (Meng et al.

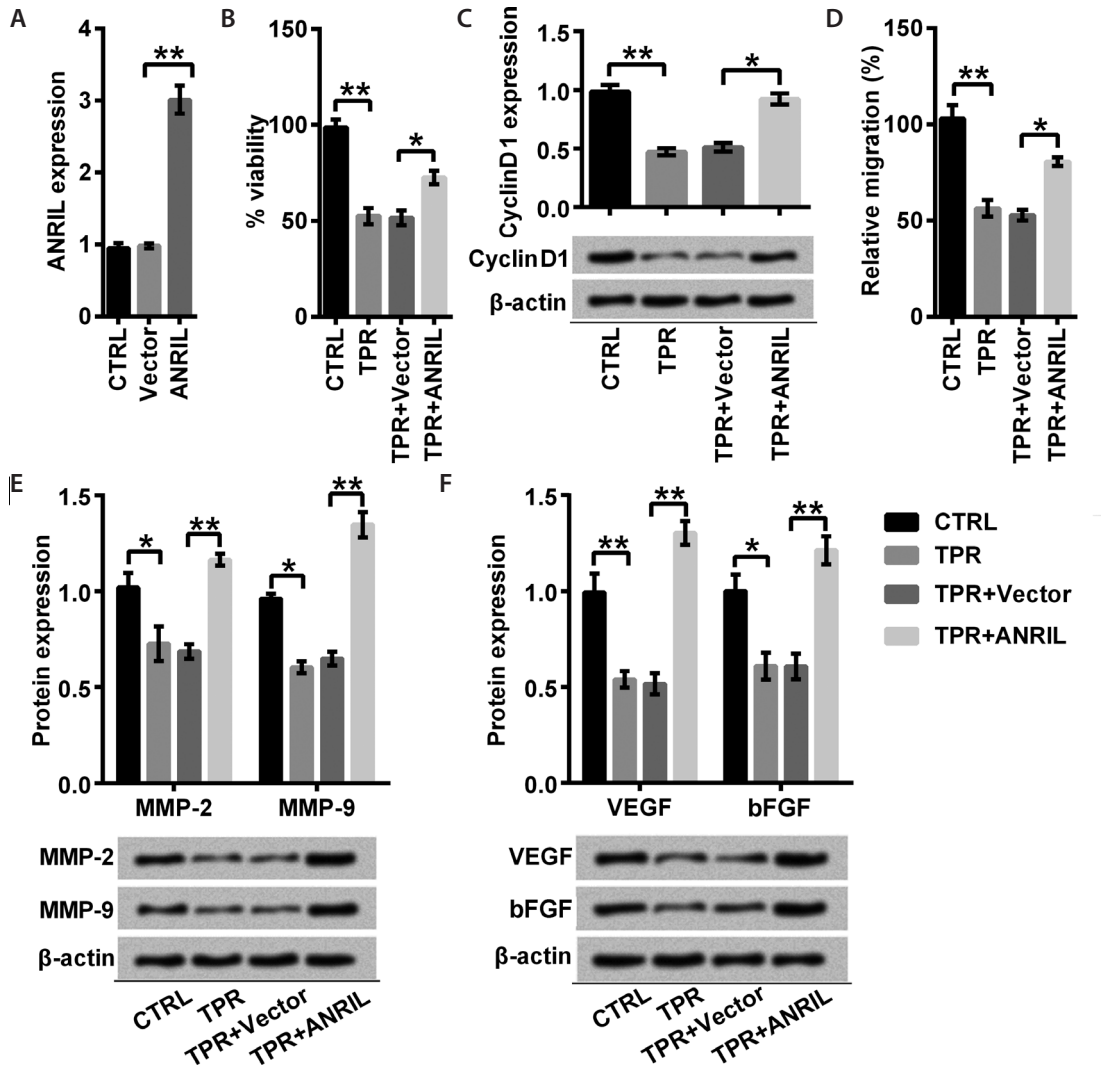

Figure 4. Effect of tripterine on the growth of *ANRIL*-overexpressed NIH/3T3 cells. NIH/3T3 cells were transfected with or without *ANRIL*, empty vector as a negative control, and then treated with 6 μM tripterine for 4 h. **A.** *ANRIL* level assayed by qRT-PCR. **B.** Cell viability evaluated by cell counting kit-8 assay. **C.** Cyclin D1 protein expression quantified by Western blot method. **D.** Migration behaviors assessed by 24-Transwell assay. MMPs (MMP-2 and MMP-9; **E**) as well as VEGF and bFGF **(F)** examined by Western blot analysis. Data represented means ± SD. * $p < 0.05$, ** $p < 0.01$. MMP, matrix metallopeptidase; VEGF, vascular endothelial growth factor; bFGF, basic fibroblast growth factor. For more abbreviations, see Fig. 3.

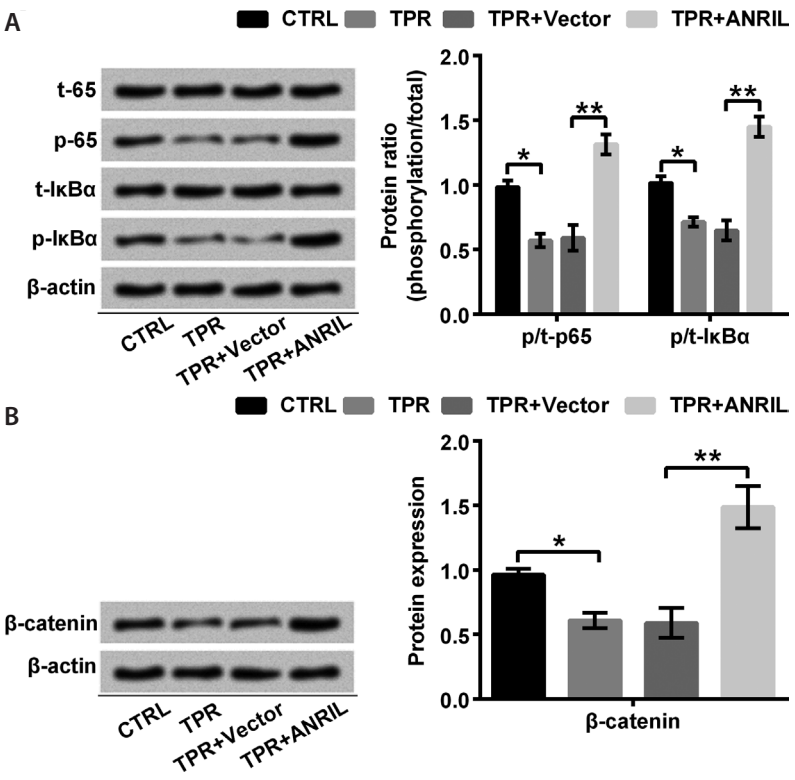

Figure 5. Effect of tripterine-mediated *ANRIL* on NF-κB and β-catenin transduction cascades. NIH/3T3 cells were transfected with or without *ANRIL*, empty vector as a negative control, and then treated with 6 μM tripterine for 4 h. Cell lysates analyzed by Western blotting with anti-p65 antibody, pSer536-p65 antibody, IκBα antibody, pSer32-IκBα antibody **(A)** and β-catenin antibody **(B)**. Data represented means ± SD after normalization with β-actin. * $p < 0.05$, ** $p < 0.01$. p, phospho; t, total; IκBα, inhibitor of nuclear factor kappa-B alpha; NF-κB, nuclear factor-kappa B. For more abbreviations, see Fig. 3.

2019). The results of our study revealed that tripterine administration has an evident effect on *ANRIL* known to participate in modulating production of ECM molecules (Thomas et al. 2018) which are crucial for scarring (Keane et al. 2018). Moreover, tripterine does suppress cell viability, block migration and blocking inflammatory pathways. The overall results suggested a striking potent of tripterine in repressing scarring.

As proved in traumatic spinal cord injury, cell cycle-related proteins are chronically enhanced and result in astroglial scar formation with chronic inflammation and even tissue loss (Wu et al. 2012). Tripterine notably repressed the accumulation of cyclin D1. Considering that cyclin D1 is a crucial activator of cell cycle activation and its ablation confers neuroprotective effects by attenuating hippocampal neuronal cell loss (Kabadi et al. 2012), we considered that cyclin D1 served as an important mediator of tripterine to play roles. Besides, we hypothesized that tripterine administration caused direct decrease of cell viability; proliferation and migration were associated with a sharp reduction in MMPs, VEGF, and bFGF. However, the anti-cell viability and anti-proliferation effects of tripterine were retarded in *ANRIL*-overexpressed cells. It might be acknowledged that *ANRIL* modulates target-genes in trans, which leads to increased cell viability (Holdt et al. 2013).

Moreover, the increase in MMP expression is associated with impaired wound healing and fibrosis, and MMP inhibition has been represented as a potential therapeutic strategy to improve tissue repair outcomes (Caley et al. 2015). Interesting, tripterine attenuates intrahepatic cholestasis of pregnancy symptoms *via* inhibiting MMP-2 and MMP-9 (Guo et al. 2018). Similarly, we found tripterine down-regulated MMP-2 and MMP-9 levels in fibroblasts. However, *ANRIL* overexpression abrogated the down-regulatory role of tripterine. A recent study found that *ANRIL* functions in tissue remodeling by modulating the expression of genes which participate in mediating ECM remodeling (Congrains et al. 2012). These results substantiated that *ANRIL* might be a mediator of tripterine in modulating MMPs expression.

VEGF-mediated angiogenic response is one of the key causative factors on hypertrophic scarring (Kwak et al. 2016). Tripterine has been identified to attenuate the secretion of VEGF and consequently suppress vascular tube formation (Huang et al. 2012). Consistently, we observed that tripterine decreased the expression of VEGF. Additionally, we found *ANRIL* overexpression contributed to the abundance of VEGF. Of particular, *ANRIL* regulates VEGF expression in mediation of specific miRs in diabetic retinopathy (Thomas et al. 2017). In this regard, it seems that through repressing *ANRIL* and subsequently mediated suppression of VEGF, tripterine favored an anti-angiogenic profile.

Besides, tripterine obviously impeded the accumulation of bFGF, which has been recognized as a critical inducer of proliferation (Choi et al. 2010) and migration (Kanazawa et al. 2010). Despite the fact that most studies confirmed that bFGF facilitates wound healing and reduces scarring (Eto et al. 2012;

Shi et al. 2013), abnormal overexpression of bFGF from fibroblasts might be implicated in the pathological fibrotic progress in hypertrophic scars (Akimoto et al. 1999), which might be ascribed to the type of fibroblasts (Song et al. 2011). What's more, bFGF might mainly function as a strong activator of proliferation and migration instead of an anti-scarring mediator. In addition, bFGF was found to be reversely up-regulated in *ANRIL*-transfected cells treated by tripterine, suggesting that tripterine weakened proliferation and migration by repressing bFGF which might be a downstream target of *ANRIL*.

Signaling transduction by NF-κB pathway is crucial for wound healing process since it mediates the expression of proteins including fibronectin, cyclin D1 and vascular endothelial growth factor (Park et al. 2018). The crucial anti-inflammatory effects of tripterine have been elucidated through NF-κB pathway (Tozawa et al. 2011). Our results on the dephosphorylation of p65 and IκBα pointed toward a blockade of NF-κB pathway by tripterine, and *ANRIL* overexpression caused the abundance of phosphorylated forms. In fibrotic skin diseases, β-catenin activation can substantially exhibit a pro-fibrotic role because it mediates the expression of target genes implicated in the pro-fibrotic effects (Hamburg et al. 2012). In spinal cord injury, the glial scarring is reduced by abrogating the signaling transduction of β-catenin pathway since the bluntness of β-catenin improves the environment which is permissive to axonal regeneration (Rodriguez et al. 2014). We found tripterine caused the inactivation of β-catenin pathway by down-regulating *ANRIL*, implying that the anti-scarring potential of tripterine might be attributed to the bluntness of β-catenin.

Ultimately, we concluded that tripterine holds important implication in anti-scarring by blunting proliferation and migration with down-regulating cyclin D1, MMPs, VEGF and bFGF. Furthermore, we consolidated that tripterine might function as an anti-scarring agent by down-regulating *ANRIL* which can block NF-κB and β-catenin pathways.

Acknowledgments. This research did not receive any specific grant from funding agencies in the public, commercial, or not-for-profit sectors.

Conflict of interest. The authors declare that there are no conflicts of interest.

Availability of data and materials. The datasets used and/or analyzed during the current study are available from the corresponding author on reasonable request.

References

Akimoto S, Ishikawa O, Iijima C, Miyachi Y (1999): Expression of basic fibroblast growth factor and its receptor by fibroblast, macrophages and mast cells in hypertrophic scar. Eur. J. Dermatol. **9,** 357-362

Anderson MA, Burda JE, Ren Y, Ao Y, O'Shea TM, Kawaguchi R, Coppola G, Khakh BS, Deming TJ, Sofroniew MV (2016): Astrocyte scar formation aids central nervous system axon regeneration. Nature **532,** 195-200 https://doi.org/10.1038/nature17623

Astry B, Venkatesha SH, Laurence A, Christensen-Quick A, Garzino-Demo A, Frieman MB, O'Shea JJ, Moudgil KD (2015): Celastrol, a Chinese herbal compound, controls autoimmune inflammation by altering the balance of pathogenic and regulatory T cells in the target organ. Clin. Immunol. **157,** 228-238 https://doi.org/10.1016/j.clim.2015.01.011

Bian M, Du X, Cui J, Wang P, Wang W, Zhu W, Zhang T, Chen Y (2016): Celastrol protects mouse retinas from bright light-induced degeneration through inhibition of oxidative stress and inflammation. J. Neuroinflammation **13,** 50 https://doi.org/10.1186/s12974-016-0516-8

Caley MP, Martins VLC, O'Toole EA (2015): Metalloproteinases and wound healing. Adv. Wound Care **4,** 225-234 https://doi.org/10.1089/wound.2014.0581

Choi JW, Kim S, Kim TM, Kim YM, Seo HW, Park TS, Jeong JW, Song G, Han JY (2010): Basic fibroblast growth factor activates MEK/ERK cell signaling pathway and stimulates the proliferation of chicken primordial germ cells. PloS One **5,** e12968 https://doi.org/10.1371/journal.pone.0012968

Congrains A, Kamide K, Katsuya T, Yasuda O, Oguro R, Yamamoto K, Ohishi M, Rakugi H (2012): CVD-associated non-coding RNA, ANRIL, modulates expression of atherogenic pathways in VSMC. Biochem. Biophys. Res. Commun. **419,** 612-616 https://doi.org/10.1016/j.bbrc.2012.02.050

Eto H, Suga H, Aoi N, Kato H, Doi K, Kuno S, Tabata Y, Yoshimura K (2012): Therapeutic potential of fibroblast growth factor-2 for hypertrophic scars: upregulation of MMP-1 and HGF expression. Lab. Inves. **92,** 214-223 https://doi.org/10.1038/labinvest.2011.127

Finnerty CC, Jeschke MG, Branski LK, Barret JP, Dziewulski P, Herndon DN (2016): Hypertrophic scarring: the greatest unmet challenge after burn injury. Lancet **388,** 1427-1436 https://doi.org/10.1016/S0140-6736(16)31406-4

Furtado MB, Nim HT, Boyd SE, Rosenthal NA (2016): View from the heart: cardiac fibroblasts in development, scarring and regeneration. Development **143,** 387-397 https://doi.org/10.1242/dev.120576

Gao Y, Zhou S, Pang L, Yang J, Li H. J, Huo X, Qian SY (2019): Celastrol suppresses nitric oxide synthases and the angiogenesis pathway in colorectal cancer. Free Radic. Res. **53,** 1-11 https://doi.org/10.1080/10715762.2019.1575512

Guo J, Wang Y, Wang N, Bai Y, Shi D (2018): Celastrol Attenuates Intrahepatic Cholestasis of Pregnancy by Inhibiting Matrix Metalloproteinases-2 and 9. Ann. Hepatol. **18,** 40-47 https://doi.org/10.5604/01.3001.0012.7860

Hamburg EJ, Atit RP (2012): Sustained beta-catenin activity in dermal fibroblasts is sufficient for skin fibrosis. J. Invest. Dermatol. **132,** 2469-2472 https://doi.org/10.1038/jid.2012.155

Holdt LM, Hoffmann S, Sass K, Langenberger D, Scholz M, Krohn K, Finstermeier K, Stahringer A, Wilfert W, Beutner F, et al. (2013): Alu elements in ANRIL non-coding RNA at chromo-

some 9p21 modulate atherogenic cell functions through trans-regulation of gene networks. PLoS Genet. **9,** e1003588 https://doi.org/10.1371/journal.pgen.1003588

Holdt LM, Stahringer A, Sass K, Pichler G, Kulak NA, Wilfert W, Kohlmaier A, Herbst A, Northoff BH, Nicolaou A, et al. (2016): Circular non-coding RNA ANRIL modulates ribosomal RNA maturation and atherosclerosis in humans. Nat. Commun. **7,** 12429 https://doi.org/10.1038/ncomms12429

Huang S, Tang Y, Cai X, Peng X, Liu X, Zhang L, Xiang Y, Wang D, Wang X, Pan T (2012): Celastrol inhibits vasculogenesis by suppressing the VEGF-induced functional activity of bone marrow-derived endothelial progenitor cells. Biochem. Biophys. Res. Commun. **423,** 467-472 https://doi.org/10.1016/j.bbrc.2012.05.143

Kabadi SV, Stoica BA, Loane DJ, Byrnes KR, Hanscom M, Cabatbat RM, Tan MT, Faden AI (2012): Cyclin D1 gene ablation confers neuroprotection in traumatic brain injury. J. Neurotrauma **29,** 813-827 https://doi.org/10.1089/neu.2011.1980

Kanazawa S, Fujiwara T, Matsuzaki S, Shingaki K, Taniguchi M, Miyata S, Tohyama M, Sakai Y, Yano K, Hosokawa K, Kubo T (2010): bFGF regulates PI3-kinase-Rac1-JNK pathway and promotes fibroblast migration in wound healing. PloS One **5,** e12228 https://doi.org/10.1371/journal.pone.0012228

Keane TJ, Horejs CM, Stevens MM (2018): Scarring vs. functional healing: Matrix-based strategies to regulate tissue repair. Advanced drug delivery reviews **129,** 407-419 https://doi.org/10.1016/j.addr.2018.02.002

Kwak DH, Bae TH, Kim WS, Kim HK (2016): Anti-vascular endothelial growth factor (bevacizumab) therapy reduces hypertrophic scar formation in a rabbit ear wounding model. Arch. Plast. Surg. **43,** 491-497 https://doi.org/10.5999/aps.2016.43.6.491

Lv QW, Zhang W, Shi Q, Zheng WJ, Li X, Chen H, Wu QJ, Jiang WL, Li HB, Gong L, et al. (2015): Comparison of Tripterygium wilfordii Hook F with methotrexate in the treatment of active rheumatoid arthritis (TRIFRA): a randomised, controlled clinical trial. Ann. Rheum. Dis. **74,** 1078-1086

Meng S, Sun L, Wang L, Lin Z, Liu Z, Xi L, Wang Z, Zheng Y (2019): Loading of water-insoluble celastrol into niosome hydrogels for improved topical permeation and anti-psoriasis activity. Colloids Surf. B. Biointerfaces **182,** 110352 https://doi.org/10.1016/j.colsurfb.2019.110352

Naemura M, Murasaki C, Inoue Y, Okamoto H, Kotake Y (2015): Long Noncoding RNA ANRIL regulates proliferation of non-small cell lung cancer and cervical cancer cells. Anticancer Res. **35,** 5377-5382

Park YR, Sultan MT, Park HJ, Lee JM, Ju HW, Lee OJ, Lee DJ, Kaplan DL, Park CH (2018): NF-kappaB signaling is key in the wound healing processes of silk fibroin. Acta Biomater. **67,** 183-195 https://doi.org/10.1016/j.actbio.2017.12.006

Rodriguez JP, Coulter M, Miotke J, Meyer RL, Takemaru K, Levine JM (2014): Abrogation of beta-catenin signaling in oligodendrocyte precursor cells reduces glial scarring and promotes axon regeneration after CNS injury. J. Neurosci. **34,** 10285-10297 https://doi.org/10.1523/JNEUROSCI.4915-13.2014

Rohani MG, Parks WC (2015): Matrix remodeling by MMPs during wound repair. Matrix Biol. **44-46,** 113-121 https://doi.org/10.1016/j.matbio.2015.03.002

Salvatore SP, Cha EK, Rosoff JS, Seshan SV (2013): Nonneoplastic renal cortical scarring at tumor nephrectomy predicts decline in kidney function. Arch. Pathol. Lab. Med. **137,** 531-540 https://doi.org/10.5858/arpa.2012-0070-OA

Shi HX, Lin C, Lin BB, Wang ZG, Zhang HY, Wu FZ, Cheng Y, Xiang LJ, Guo DJ, Luo X, et al. (2013): The anti-scar effects of basic fibroblast growth factor on the wound repair in vitro and in vivo. PloS One **8,** e59966 https://doi.org/10.1371/journal.pone.0059966

Sidgwick GP, Bayat A (2012): Extracellular matrix molecules implicated in hypertrophic and keloid scarring. J. Eur. Dermatol. Venereol. **26,** 141-152 https://doi.org/10.1111/j.1468-3083.2011.04200.x

Song R, Bian HN, Lai W, Chen HD, Zhao KS (2011): Normal skin and hypertrophic scar fibroblasts differentially regulate collagen and fibronectin expression as well as mitochondrial membrane potential in response to basic fibroblast growth factor. Braz. J. Med. Biol. Res. **44,** 402-410 https://doi.org/10.1590/S0100-879X2011000500004

Thomas AA, Feng B, Chakrabarti S (2017): ANRIL: A Regulator of VEGF in Diabetic Retinopathy. Invest. Ophthalmol. Vis. Sci. **58,** 470-480 https://doi.org/10.1167/iovs.16-20569

Thomas AA, Feng B, Chakrabarti S (2018): ANRIL regulates production of extracellular matrix proteins and vasoactive factors in diabetic complications. Am. J. Physiol. Endocrinol. Metab. **314,** E191-e200 https://doi.org/10.1152/ajpendo.00268.2017

Tozawa K, Sagawa M, Kizaki M (2011): Quinone methide tripterine, celastrol, induces apoptosis in human myeloma cells via NF-kappaB pathway. Int. J. Oncol. **39,** 1117-1122

Verma SM, Okawa J, Propert KJ, Werth VP (2014): The impact of skin damage due to cutaneous lupus on quality of life. Br. J. Dermatol. **170,** 315-321 https://doi.org/10.1111/bjd.12653

Wu J, Pajoohesh-Ganji A, Stoica BA, Dinizo M, Guanciale K, Faden AI (2012): Delayed expression of cell cycle proteins contributes to astroglial scar formation and chronic inflammation after rat spinal cord contusion. J. Neuroinflammation **9,** 169 https://doi.org/10.1186/1742-2094-9-169

Zhou X, Han X, Wittfeldt A, Sun J, Liu C, Wang X, Gan L. M, Cao H, Liang Z (2016): Long non-coding RNA ANRIL regulates inflammatory responses as a novel component of NF-kappaB pathway. RNA Biol. **13,** 98-108 https://doi.org/10.1080/15476286.2015.1122164

Zhou YZ, Zhao LD, Chen H, Zhang Y, Wang DF, Huang LF, Lv QW, Liu B, Li Z, Wei W, et al. (2018): Comparison of the impact of Tripterygium wilfordii Hook F and Methotrexate treatment on radiological progression in active rheumatoid arthritis: 2-year follow up of a randomized, non-blinded, controlled study. Arthritis Res. Ther. **20,** 70 https://doi.org/10.1186/s13075-018-1563-6

Received: April 30, 2019
Final version accepted: November 4, 2019